

# Phase Balancing Using Energy Storage in Power Grids under Uncertainty

Sun Sun, *Student Member, IEEE*, Ben Liang, *Senior Member, IEEE*, Min Dong, *Senior Member, IEEE*, and Joshua A. Taylor, *Member, IEEE*

**Abstract**—Phase balancing is essential to safe power system operation. We consider a substation connected to multiple phases, each with single-phase loads, generation, and energy storage. A representative of the substation operates the system and aims to minimize the cost of all phases and to balance loads among phases. We first consider ideal energy storage with lossless charging and discharging, and propose both centralized and distributed real-time algorithms taking into account system uncertainty. The proposed algorithm does not require any system statistics and asymptotically achieves the minimum system cost with large energy storage. We then extend the algorithm to accommodate more realistic non-ideal energy storage that has imperfect charging and discharging. The performance of the proposed algorithm is evaluated through extensive simulation and compared with that of a benchmark greedy algorithm. Simulation shows that our algorithm leads to strong performance over a wide range of storage characteristics.

**Index Terms**—Distributed algorithm, energy storage, phase balancing, stochastic optimization.

## I. INTRODUCTION

In North America, many residential customers are connected to distribution systems through single-phase lines. Phase balancing, i.e., maintaining the balance of loads among phases, is crucial for power grid operation [1]. This is because phase imbalance can increase energy losses and the risk of failures, and can also degrade system power quality. With the spread of single-phase renewable generators, such as wind and solar generators, and large loads, such as electric vehicles, phase imbalance could be aggravated and thus deserves more careful study. For example, the impact of integration of electric vehicles on phase imbalance was investigated in [2].

Previous works on phase balancing have considered methods such as phase swapping (e.g., [3]) and feeder reconfiguration (e.g., [4]). However, these approaches can be ineffective or can incur extra costs on human resources, maintenance expenses, and planned outage duration [3]. An alternative method is to employ energy storage to mitigate the imbalance among phases, which is the focus of this paper.

Energy storage has been used widely in power grids for applications such as energy arbitrage, regulation, and load following [5]. Examples of single-phase storage include:

- Traditional standalone storage such as batteries, flywheels, etc [6].

Sun Sun, Ben Liang, and Joshua A. Taylor are with the Department of Electrical and Computer Engineering, University of Toronto, Toronto, Ontario M5S 3G4 (email: {ssun, liang}@comm.utoronto.ca, josh.taylor@utoronto.ca).

Min Dong is with the Department of Electrical Computer and Software Engineering, University of Ontario Institute of Technology, Oshawa, Ontario L1H 7K4 (email: min.dong@uoit.ca).

This work was supported by the Natural Sciences and Engineering Research Council (NSERC) of Canada under Discovery Grants RGPIN-2014-05181 and RGPIN-2015-05506.

- Batteries in single-phase connected buildings such as plug-in electric vehicles [7].
- Aggregations of small single-phase deferrable loads, e.g., residential thermostatically controlled loads or electric vehicle garages, which have been shown to be representable as equivalent storage [8]–[10].

The control of energy storage for power grid applications is, however, generally a challenging problem due to storage characteristics as well as system uncertainty. There are many existing works on storage control in power grids. For example, using stochastic dynamic programming, the authors of [11] proposed a stationary optimal policy for power balancing, and the authors of [12] investigated both optimal and suboptimal policies for energy balancing. Nevertheless, the derivation of an optimal policy under dynamic programming generally relies on system statistics and some specific form of the problem structure, and therefore it cannot be easily extended. Similarly, the authors of [13] considered stochastic model predictive control. However, the algorithm performance can only be evaluated through numerical examples.

Besides the above two approaches, several recent works have employed Lyapunov optimization [14] for energy storage control. In particular, the authors of [15] investigated a power-cost minimization problem in data centers with energy storage, and were the first to use the technique of Lyapunov optimization for real-time storage control. The technique was then employed in several subsequent works to design energy storage control for various applications in grid operation, such as power balancing [16], [17], demand side management [18], [19], and EV charging [20]. Furthermore, the authors of [21] analyzed the trade-off between averaging out the energy fluctuation across time and across space, the authors of [22] studied generalized storage control with general cost functions, and the authors of [23] investigated the management of networked storage with a DC power flow model. Among these works, single storage control was considered in [15], [18], and [22]. For multiple storage control, charging efficiency was incorporated into the storage model in [20], both charging and discharging efficiencies were introduced in [16], and storage efficiency that models the energy loss over time was included in [19].

In this paper, we study the problem of phase balancing with energy storage in the presence of system uncertainty. Unlike prior works such as [24] and [25] that focus on heuristic algorithms for storage control in phase balancing, in this paper, we provide efficient algorithms with strong theoretical performance guarantee. We consider a substation connected to multiple phases, each with single-phase uncontrollable flow, controllable flow, and energy storage. In particular, we consider phase balancing on a time scale of seconds to

minutes. As such, we do not model power system physics such as frequency and voltage magnitude. Aiming at minimizing the cost of all phases and mitigating phase imbalance, we propose a real-time algorithm that can be easily implemented by the substation. Moreover, for the likely scenario of limited communication between the substation and each phase, we provide a distributed implementation of the real-time algorithm where only limited information exchange is required.

The main contributions of this paper are summarized as follows. First, we formulate a stochastic optimization problem for phase balancing incorporating system uncertainty, storage characteristics, and power network constraints. Second, for ideal energy storage with lossless charging and discharging, we provide a real-time algorithm building on the framework of Lyapunov optimization and prove its analytical performance guarantee. Moreover, we offer distributed implementation of the algorithm with fast convergence. Third, we extend the algorithm to accommodate non-ideal energy storage with imperfect charging and discharging efficiency and show its analytical performance. Finally, to numerically evaluate the performance of the proposed algorithm, we compare it with a benchmark greedy algorithm under various settings and parameters. Simulation reveals that our proposed algorithm is competitive in general. In particular, the proposed algorithm has strong performance when applied to storage with a large energy capacity, a high value of the energy-power ratio (e.g., compressed air energy storage and batteries), and moderate-to-high charging and discharging efficiency (e.g., the round-trip efficiency of storage is greater than 65%). In addition, a practical outcome of our analysis shows the following design guideline: optimal power balancing favors even allocation of storage capacity over the phases.

Our paper is technically most similar to [23], in which a distributed real-time algorithm is proposed for power grids with energy storage. However, these two papers are different in terms of the application, objective, communication topology, and power network constraints. Hence, the problem formulation and the design of distributed implementation are largely different. Moreover, for analysis, charging and discharging efficiencies were not considered in the storage model in [23]. While the authors stated that their framework could further incorporate imperfect charging and discharging, no implementable algorithm was given to address that. In contrast, in this paper, we provide an efficient algorithm to deal with imperfect charging and discharging.

A preliminary version of this work has been presented in [26]. In this paper, we significantly extend [26] in two ways: analytically, for the proposed algorithms, we provide more in-depth performance analysis for both ideal and non-ideal storage; numerically, we implement extensive simulation by examining various storage characteristics and the effect of correlation between the phases' random power imbalances.

The remainder of this paper is organized as follows. In Section II, we describe the system model and formulate the optimization problem. In Section III, we propose both centralized and distributed real-time algorithms for ideal energy storage. In Section IV, we extend the algorithm to accommodate non-ideal energy storage with imperfect charging and discharging.

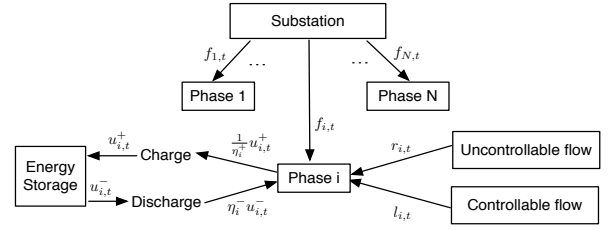


Fig. 1. System model with  $N$  phases. The details of the  $i$ -th phase are shown.

Numerical results are presented in Section V, and we conclude in Section VI.

## II. SYSTEM MODEL AND PROBLEM STATEMENT

Consider a discrete-time model with time  $t \in \{0, 1, 2, \dots\}$ . To simplify notation, we normalize the duration of each time period  $\Delta t$  to one and thus eliminate  $\Delta t$  in presentation. The system model is depicted in Fig. 1. A substation is connected with  $N \geq 2$  phases, each with single-phase loads and generation.<sup>1</sup> We consider a general case where it is optional for each phase to deploy energy storage. Denote the set of phases that deploy storage by  $\mathcal{E} \subseteq \{1, 2, \dots, N\}$ . Below we first describe the components of each phase.

### A. System Model of Each Phase

At the  $i$ -th phase, denote the amount of uncontrollable power at time slot  $t$  by  $r_{i,t}$ . The uncontrollable flow can represent renewable generation such as wind and solar, base loads, or the difference between renewable generation and base loads. Since the uncontrollable flow is generally governed by nature or uncertain human behavior, we assume that  $r_{i,t}$  is random, but it is confined within an interval  $[r_{i,\min}, r_{i,\max}]$ . Throughout the paper we use a bold letter to denote a vector that contains elements of  $N$  phases. Here, we define  $\mathbf{r}_t \triangleq [r_{1,t}, \dots, r_{N,t}]$  to represent the uncontrollable flow vector at time slot  $t$ . The other vectors in the rest of this paper are defined similarly.

Denote the amount of the controllable power flow at the  $i$ -th phase at time  $t$  by  $l_{i,t}$ . The controllable flow can represent the output of conventional generators, or the consumption of flexible loads. We associate a cost function with the controllable flow and denote the function by  $C_i(l_{i,t})$ , which can represent the cost of local generators (e.g., an on-site diesel generator), or the cost of a utility for consuming power.

Denote the power flow between the substation and the  $i$ -th phase at time slot  $t$  by  $f_{i,t}$ . Due to the capacity constraints of power lines, the value of  $f_{i,t}$  is generally confined. We assume that at each time slot the power flow vector  $\mathbf{f}_t \in \mathcal{F}$ , where the set  $\mathcal{F}$  is non-empty, compact, and convex. For example,  $\mathcal{F}$  may be defined as  $\mathcal{F} \triangleq \{\mathbf{f}_t | f_{i,t} \in [f_{i,\min}, f_{i,\max}], \forall i\}$ .

**Remark:** The values of  $r_{i,t}$ ,  $l_{i,t}$ , and  $f_{i,t}$  can be positive or negative. We use the positive sign to indicate power injection

<sup>1</sup>In practice, a typical substation consists of one or more three-phase feeders connected through a feeder breaker, each of which can supply multiple single-phase loads. In this paper, since we focus on the problem of phase balancing in one feeder, the structure of feeders is omitted in Fig. 1. For a more thorough description of a distribution substation, please see Chapter 1 in [27].

into the  $i$ -th phase, and the negative sign to indicate power extraction from the  $i$ -th phase.

Assume that the  $i$ -th phase is equipped with an energy storage unit, i.e.,  $i \in \mathcal{E}$ . Denote the charging and discharging rates of the storage at time slot  $t$  by  $u_{i,t}^+ \in [0, u_{i,\max}]$  and  $u_{i,t}^- \in [0, u_{i,\max}]$ , respectively, where  $u_{i,\max}$  is the maximum charging and discharging rates. Denote the energy state of the  $i$ -th storage at the beginning of time slot  $t$  by  $s_{i,t}$ , which evolves as  $s_{i,t+1} = s_{i,t} + u_{i,t}^+ - u_{i,t}^-$ . The energy state  $s_{i,t}$  is required to be within the storage's capacity limits  $[s_{i,\min}, s_{i,\max}]$ .

Due to conversion and storage losses, charging and discharging may not be perfectly efficient. For the  $i$ -th storage, we denote the charging efficiency by  $\eta_i^+ \in (0, 1]$  and the discharging efficiency by  $\eta_i^- \in (0, 1]$ . Then, the associated charging and discharging quantities seen on each phase are  $\frac{1}{\eta_i^+} u_{i,t}^+$  and  $\eta_i^- u_{i,t}^-$ , respectively (see Fig. 1). Owing to the round-trip efficiency or other operating constraints, simultaneous charging and discharging may be forbidden in practice, which can be reflected by the constraint  $u_{i,t}^+ \cdot u_{i,t}^- = 0, i \in \mathcal{E}$ . Moreover, if the  $i$ -th phase is not equipped with storage, i.e.,  $i \notin \mathcal{E}$ , we simply set the values of  $s_{i,t}, u_{i,t}^+$ , and  $u_{i,t}^-$  to zero.

The energy storage can additionally be used for arbitrage.<sup>2</sup> Denote the electricity price at time slot  $t$  by  $p_t \in [p_{\min}, p_{\max}]$ , which is random over time. Then the cost of the  $i$ -th phase for energy arbitrage during time slot  $t$  is  $p_t(\frac{1}{\eta_i^+} u_{i,t}^+ - \eta_i^- u_{i,t}^-)$ . Finally, frequent charging and discharging can shorten the lifetime of storage [28]. To model this effect, we introduce a degradation cost function  $D_i(\cdot)$ , with negative input indicating discharging and positive input indicating charging. Therefore, the degradation cost incurred at time slot  $t$  is given by  $D_i(u_{i,t}^+) + D_i(-u_{i,t}^-)$ .<sup>3</sup>

## B. Problem Statement

Since phase imbalance is harmful for power system operation, it is critical to balance the power flows  $f_{i,t}$  among phases. To this end, we introduce a loss function  $F(\cdot)$  to characterize the deviation of  $f_{i,t}$  from the average power flow. In particular, for the  $i$ -th phase,  $F(\cdot)$  is a function of  $f_{i,t} - \bar{f}_t$ , where  $\bar{f}_t$  is the average defined as  $\bar{f}_t \triangleq \frac{1}{N} \sum_{j=1}^N f_{j,t}$ .

We assume that the system is operated by a representative of the substation, who aims to minimize the long-term system cost, which includes the costs of all phases. Specifically, based on the model described in Section II-A, the system cost at time slot  $t$  is given by

$$w_t = \sum_{i \in \mathcal{E}} \left[ p_t \left( \frac{1}{\eta_i^+} u_{i,t}^+ - \eta_i^- u_{i,t}^- \right) + D_i(u_{i,t}^+) + D_i(-u_{i,t}^-) \right] + \sum_{i=1}^N [C_i(l_{i,t}) + F(f_{i,t} - \bar{f}_t)].$$

<sup>2</sup>Energy storage is still expensive based on the current technology. Therefore, in practice, besides phase balancing and energy arbitrage, energy storage can be used to provide other grid-wide services, e.g., volt-var control, load following, and peak shaving.

<sup>3</sup>Accurate modeling of battery degradation is highly complicated and is an active research area. In this paper, to focus on storage control, we employ a simplified degradation model, which is a function of the charging and discharging amount.

Denote the random system state at time slot  $t$  by  $\mathbf{q}_t \triangleq [\mathbf{r}_t, p_t]$ , which includes the uncontrollable power flow of  $N$  phases and the electricity price. Denote the control action at time slot  $t$  by  $\mathbf{a}_t \triangleq [l_t, \mathbf{u}_t^+, \mathbf{u}_t^-, \mathbf{f}_t]$ , which contains the controllable power flow, the charging and discharging amounts, and the power flow between each phase and the substation. We formulate the problem for phase balancing as the following stochastic optimization problem.

$$\begin{aligned} \mathbf{P1}: \quad & \min_{\{\mathbf{a}_t\}} \limsup_{T \rightarrow \infty} \frac{1}{T} \sum_{t=0}^{T-1} \mathbb{E}[w_t] \\ \text{s.t.} \quad & 0 \leq u_{i,t}^+, u_{i,t}^- \leq u_{i,\max}, \forall i \in \mathcal{E}, t, & (1) \\ & u_{i,t}^+ \cdot u_{i,t}^- = 0, \forall i \in \mathcal{E}, t, & (2) \\ & s_{i,t+1} = s_{i,t} + u_{i,t}^+ - u_{i,t}^-, \forall i \in \mathcal{E}, t, & (3) \\ & s_{i,\min} \leq s_{i,t} \leq s_{i,\max}, \forall i \in \mathcal{E}, t, & (4) \\ & u_{i,t}^- = u_{i,t}^+ = 0, \forall i \notin \mathcal{E}, t, & (5) \\ & \mathbf{f}_t \in \mathcal{F}, \forall t, & (6) \\ & f_{i,t} + r_{i,t} + l_{i,t} + \eta_i^- u_{i,t}^- - \frac{1}{\eta_i^+} u_{i,t}^+ = 0, \forall i, t. & (7) \end{aligned}$$

The expectation on the objective is taken over the randomness of  $\mathbf{q}_t$  and the possibly random control action that depends on  $\mathbf{q}_t$ . Constraint (7) enforces power balance at each phase at each time slot.

To keep mathematical exposition simple, we assume that the cost functions  $C_i(\cdot)$  and  $D_i(\cdot)$  are continuously differentiable and convex. This assumption is realistic because many practical cost functions are well approximated this way [29]. In particular, by convexity, the marginal cost is increasing. With the objective of minimizing the system cost, for the function  $C(\cdot)$ , this property discourages excessive use of the controllable flow. For battery degradation, it is understood that faster charging or discharging has a more detrimental effect on the battery lifetime, and the convexity of  $D(\cdot)$  reflects this behavior. Denote the derivatives of  $C_i(\cdot)$  and  $D_i(\cdot)$  by  $C_i'(\cdot)$  and  $D_i'(\cdot)$ , respectively. Since the variables  $u_{i,t}^+, u_{i,t}^-$ , and  $l_{i,t}$  are bounded based on the constraints of **P1**, the cost functions and their derivatives are bounded in the feasible set. For the cost function  $C_i(\cdot)$ , we denote its range by  $[C_{i,\min}, C_{i,\max}]$  and its range of the derivative by  $[C_{i,\min}', C_{i,\max}']$  in the feasible set. The range of the cost function  $D_i(\cdot)$  and that of its derivative are defined similarly. In addition, we assume that the loss function  $F(\cdot)$  is convex and continuously differentiable.

We are interested in designing both centralized and distributed real-time algorithms for solving **P1**. Distributed implementation is motivated by the limited capability of real-time communication between the substation and each phase, and also the potential privacy concerns of each phase. This is a challenging task due to system uncertainty, the coupling of all phases through the objective and constraints, and the energy state constraint (4) which couples the charging and discharging actions over time. In addition, we assume that the system is not equipped with any forecaster and only has historical information of the system states. Designing appropriate forecasters and incorporating forecast into optimal control are important directions and are left for future work.

### III. REAL-TIME ALGORITHM FOR IDEAL ENERGY STORAGE

For tractability, in this section we first consider ideal energy storage that has perfectly efficient charging and discharging, i.e.,  $\eta_i^+ = \eta_i^- = 1$ . The case of non-ideal energy storage is studied in Section IV. We first propose a centralized real-time algorithm that can be implemented by the substation and show its analytical performance. Then we provide distributed implementation for the proposed algorithm where only limited information exchange is needed.

#### A. Centralized Real-Time Algorithm and Analysis

Under perfectly efficient charging and discharging, without loss of generality, we can combine the charging and discharging variables  $u_{i,t}^+$  and  $u_{i,t}^-$  into one by introducing a new variable  $u_{i,t} \triangleq u_{i,t}^+ - u_{i,t}^-$ , which can represent the net charging and discharging amount. In particular, if  $u_{i,t} > 0$  it indicates charging, and if  $u_{i,t} < 0$  it indicates discharging.

With the new variable  $u_{i,t}$ , the non-simultaneous charging and discharging constraint (2) can be eliminated, and the evolution of the energy state amounts to  $s_{i,t+1} = s_{i,t} + u_{i,t}$ . In addition, with  $u_{i,t}$ , the control action at time slot  $t$  is now  $\mathbf{a}_t \triangleq [\mathbf{l}_t, \mathbf{u}_t, \mathbf{f}_t]$ , and the system cost can be rewritten as  $w_t = \sum_{i \in \mathcal{E}} [p_t u_{i,t} + D_i(u_{i,t})] + \sum_{i=1}^N [C_i(l_{i,t}) + F(f_{i,t} - \bar{f}_t)]$ .

For the design of real-time implementation, we employ Lyapunov optimization [14], which has been used widely in wireless networks for dealing with time-averaged constraints and providing simple yet efficient algorithms for complex dynamic systems. However, the energy state constraint (4) is not a time-averaged constraint but a hard constraint, and it couples the control action  $u_{i,t}$  over multiple time instances. As a result, **P1** is not amenable to the standard framework of Lyapunov optimization. To overcome this difficulty, we replace the energy state constraints (3) and (4) with a new time-averaged constraint, which only requires the net charging and discharging amount to be zero on average, i.e.,

$$\lim_{T \rightarrow \infty} \frac{1}{T} \sum_{t=0}^{T-1} \mathbb{E}[u_{i,t}] = 0, \forall i \in \mathcal{E}. \quad (8)$$

With the new constraint (8), we form a new stochastic optimization problem as follows:

$$\begin{aligned} \mathbf{P2}: \quad & \min_{\{\mathbf{a}_t\}} \limsup_{T \rightarrow \infty} \frac{1}{T} \sum_{t=0}^{T-1} \mathbb{E}[w_t] \\ & \text{s.t.} \quad (6), (8), \\ & f_{i,t} + r_{i,t} + l_{i,t} - u_{i,t} = 0, \forall i, t, \quad (9) \\ & u_{i,t} = 0, \forall i \notin \mathcal{E}, t, \quad (10) \\ & -u_{i,\max} \leq u_{i,t} \leq u_{i,\max}, \forall i \in \mathcal{E}, t. \quad (11) \end{aligned}$$

It can be shown that constraints (3) and (4) imply (8), i.e., any  $u_{i,t}$  that satisfies (3) and (4) also satisfies (8). Hence, **P2** is a relaxation of **P1** (see Appendix A).

The above relaxation step is crucial for applying Lyapunov optimization. However, we emphasize that, solving **P2** is not our purpose (it is clear that, due to the relaxation of constraints (3) and (4), a solution to **P2** may be infeasible to **P1**).

Instead, the significance of proposing **P2** is to facilitate the development of a real-time algorithm for **P1** and the associated performance analysis. Later we will prove in Proposition 1 that our proposed algorithm ensures that constraints (3) and (4) are satisfied, and therefore produces a feasible solution to **P1**.

We now propose a real-time algorithm leveraging Lyapunov optimization techniques. At time slot  $t$ , for phase  $i \in \mathcal{E}$ , define a Lyapunov function  $L(s_{i,t}) \triangleq \frac{1}{2}(s_{i,t} - \beta_i)^2$ , which measures the deviation of the energy state  $s_{i,t}$  from a perturbation parameter  $\beta_i$ . The parameter  $\beta_i$  is introduced to ensure the boundedness of the energy state, i.e., constraint (4), and it needs to be carefully designed. In addition, we define a one-slot conditional Lyapunov drift as  $\Delta(s_t) \triangleq \mathbb{E} \left[ \sum_{i \in \mathcal{E}} \frac{L(s_{i,t+1}) - L(s_{i,t})}{V_i} | s_t \right]$ , which collects a weighted sum of the one-slot conditional drifts of the Lyapunov functions for all phases with storage.

In our design of the real-time algorithm, instead of directly minimizing the system cost  $w_t$ , we consider a drift-plus-cost function  $\Delta(s_t) + \mathbb{E}[w_t | s_t]$ . In particular, we first derive an upper bound on the drift-plus-cost function (see Appendix B for the upper bound), and then formulate a per-slot optimization problem to minimize this upper bound. Consequently, at each time slot  $t$ , we solve the following optimization problem:

$$\mathbf{P3}: \quad \min_{\mathbf{a}_t} w_t + \sum_{i \in \mathcal{E}} \frac{(s_{i,t} - \beta_i)u_{i,t}}{V_i} \quad \text{s.t.} \quad (5) - (7), (11).$$

Denote an optimal solution of **P3** at time slot  $t$  by  $\mathbf{a}_t^* \triangleq [\mathbf{l}_t^*, \mathbf{u}_t^*, \mathbf{f}_t^*]$ . At each time slot, after obtaining the solution  $\mathbf{a}_t^*$ , we update  $s_{i,t}$  using  $u_{i,t}^*$ . It can be easily verified that the optimization problem **P3** is convex, and thus can be solved by standard convex optimization software packages such as those in MATLAB. We will later shown in Theorem 1 that such design of the per-slot optimization problem leads to certain guaranteed performance.

In the proposition below, we show that, despite the relaxation to arrive at **P2**, by appropriately designing the perturbation parameter  $\beta_i$ , we can ensure that constraint (4) is satisfied, and therefore the control actions  $\{\mathbf{a}_t^*\}$  are feasible to **P1**.

*Proposition 1:* For phase  $i \in \mathcal{E}$ , set the perturbation parameter  $\beta_i$  as

$$\beta_i \triangleq s_{i,\min} + u_{i,\max} + V_i(p_{\max} + D'_{i,\max} + C'_{i,\max}) \quad (12)$$

where  $V_i \in (0, V_{i,\max}]$  with

$$V_{i,\max} \triangleq \frac{s_{i,\max} - s_{i,\min} - 2u_{i,\max}}{p_{\max} - p_{\min} + D'_{i,\max} - D'_{i,\min} + C'_{i,\max} - C'_{i,\min}}. \quad (13)$$

Then the control actions  $\{\mathbf{a}_t^*\}$  obtained by solving **P3** at each time  $t$  are feasible to **P1**.

*Proof:* See Appendix C. ■

To ensure the positivity of  $V_{i,\max}$  in (13), we need the numerator  $s_{i,\max} - s_{i,\min} - 2u_{i,\max} > 0$ . This is generally true for real-time applications, in which the length of each time interval is small ranging from a few seconds to minutes.

The overall centralized real-time algorithm is summarized in Algorithm 1, which can be implemented by the substation. It is worth mentioning that the proposed algorithm does not require any system statistics, which may be desirable when accurate system statistics are difficult to obtain.

---

**Algorithm 1** Centralized algorithm for ideal storage.
 

---

At time slot  $t$ , the substation executes the following steps sequentially:

- 1: observe the system state  $\mathbf{q}_t$  and the energy state  $s_{i,t}$ ;
  - 2: solve **P3** and obtain a solution  $\mathbf{a}_t^* \triangleq [\mathbf{l}_t^*, \mathbf{u}_t^*, \mathbf{f}_t^*]$ ; and
  - 3: update  $s_{i,t+1}$  by  $s_{i,t} + u_{i,t}^*$ .
- 

Denote the optimal objective value of **P1** by  $w^{\text{opt}}$ . Under Algorithm 1, denote the objective value of **P1** by  $w^*$  and the system cost at time slot  $t$  by  $w_t^*$ . The performance of Algorithm 1 is stated in the following theorem.

*Theorem 1:* Assume that the system state  $\mathbf{q}_t$  is i.i.d. over time and the equipped storage at the phases is perfectly efficient. Under Algorithm 1 the following statements hold.

- 1)  $w^* - w^{\text{opt}} \leq \sum_{i \in \mathcal{E}} \frac{u_{i,\max}^2}{2V_i}$ .
- 2)  $\frac{1}{T} \sum_{t=0}^{T-1} \mathbb{E}[w_t^*] - w^{\text{opt}} \leq \sum_{i \in \mathcal{E}} \frac{u_{i,\max}^2}{2V_i} + \frac{\mathbb{E}[L(s_{i,0})]}{TV_i}$ .

*Proof:* See Appendix D. ■

**Remarks:**

- For Theorem 1.1, first, if  $\mathcal{E}$  is empty, i.e., no phase deploys storage, then Algorithm 1 achieves the optimal objective value. In fact, for this case, Algorithm 1 reduces to a greedy algorithm that only minimizes the current system cost at each time. Second, if  $\mathcal{E}$  is non-empty, to minimize the gap to the optimal objective value, we should set  $V_i = V_{i,\max}$ . Asymptotically, if the energy capacity  $s_{i,\max}$  is large and thus  $V_{i,\max}$  is large, Algorithm 1 achieves the optimal objective value.<sup>4</sup>
- In Theorem 1.2, we characterize the performance of Algorithm 1 over a finite time horizon. The result not only shows the performance gap of the algorithm over a finite time  $T$ , but also reveals how the gap converges asymptotically to the one in Theorem 1.1 as  $T$  grows. It can be seen that, the gap contains a component  $\sum_{i \in \mathcal{E}} \frac{\mathbb{E}[L(s_{i,0})]}{TV_i}$  due to the initialization of the energy states, which linearly decreases with the time horizon  $T$ .
- The i.i.d. assumption of the system state  $\mathbf{q}_t$  can be relaxed to accommodate  $\mathbf{q}_t$  that follows a finite state irreducible and aperiodic Markov chain. Using a multi-slot drift technique [14], we can show similar conclusions which are omitted here. In simulation, we will evaluate the algorithm performance when the uncontrollable power flows are temporally correlated.

An interesting additional consequence of Theorem 1 is that we obtain a general rule of thumb for the allocation of energy storage capacity among the phases. In particular, in the following proposition, we demonstrate that, under some mild conditions, equal allocation of a given energy storage capacity results in a lower overall system cost.

*Proposition 2:* Assume that  $s_{i,\min}, u_{i,\min}$  and  $D_{i,\max} - D_{i,\min}$  are identical for all  $i \in \mathcal{E}$ . Assume further that for all phases,  $C'_{i,\max} - C'_{i,\min}$  is the same. Then, under Algorithm 1, if the total energy storage capacity  $\sum_{i \in \mathcal{E}} s_{i,\max}$  is fixed

<sup>4</sup>The choice of  $V_i = V_{i,\max}$  and the asymptotic optimality are based on the linear storage model in (3). These conclusions need to be re-examined when a more general storage model with other factors such as storage efficiency is considered [22], [23].

and the control parameter  $V_i = V_{i,\max}$  is as in (13), the upper bound of the performance gap in Theorem 1.1, i.e.,  $\sum_{i \in \mathcal{E}} \frac{u_{i,\max}^2}{2V_i}$ , is minimized when the energy storage capacity is equally allocated among phases.

*Proof:* See Appendix E. ■

The above result states that energy storage is best allocated equally over the phases. Note that this result is robust because it does not depend on any system statistics or specific values of system parameters. We will revisit this in simulation.

In this paper, as our focus is on designing real-time algorithms for storage control, we use a stylized system model shown in Fig. 1. In particular, we do not model the network structure at each phase, and therefore do not consider how to place storage. Instead, we assume a given arbitrary deployment of storage at any location of each phase. Nonetheless, we point out that storage placement affects the investment strategy of power systems and is crucial for grid operation. This problem has attracted considerable attention and has been investigated in many papers (e.g., [30]). In particular, in the case of physical storage, the authors of [30] proved that, under some technical conditions, there always exists an optimal strategy of storage placement that assigns zero storage at generation-only buses that link to the rest of the network via single transmission lines. Moreover, if storage is load aggregation, then it can be distributed over the phase. How to extend our results to consider storage placement is a topic for future study.

### B. Distributed Implementation of Centralized Algorithm

To accomplish the implementation of Algorithm 1 in a centralized way, each phase has to provide all information that is required to solve the real-time problem **P3**. Specifically, for each phase, the cost functions and the associated optimization constraints need to be communicated to the substation in advance. In addition, at each time slot, the information of the uncontrollable power flow as well as the storage energy state has to be sent to the substation. However, in practice, due to the limited capability of real-time communication along with potential privacy concerns of each phase, some of the aforementioned information may be unavailable at the substation. Therefore, the centralized implementation may be infeasible. In this subsection, we provide a distributed algorithm for solving **P3** in which only limited information exchange is required. For ease of notation, we suppress the time index  $t$  in the following presentation.

The distributed algorithm is based on the alternating direction method of multipliers (ADMM) [31]. To facilitate algorithm development, we rewrite **P3** as follows:

$$\begin{aligned}
 \min_{\mathbf{a}} \quad & \mathbf{1}(\mathbf{f} \in \mathcal{F}) + \sum_{i=1}^N \left[ H_i(l_i, u_i) + F(f_i - \bar{f}) \right] \\
 \text{s.t.} \quad & f_i + r_i + l_i - u_i = 0, \forall i
 \end{aligned} \tag{14}$$

where  $\mathbf{1}(\cdot)$  is the indicator function that equals 0 (resp.  $+\infty$ ) when the enclosed event is true (resp. false), and for each

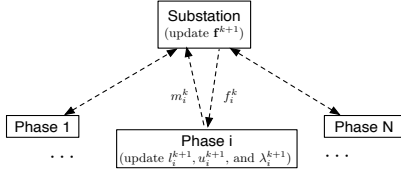


Fig. 2. Distributed implementation for solving **P3**.

phase the function  $H_i(l_i, u_i)$  is defined as follows:

$$H_i(l_i, u_i) \triangleq \begin{cases} \frac{(s_i - \beta_i)u_i}{V_i} + pu_i + D_i(u_i) + C_i(l_i) \\ + \mathbf{1}(-u_{i,\max} \leq u_i \leq u_{i,\max}), & \text{if } i \in \mathcal{E} \\ C_i(l_i) + \mathbf{1}(u_i = 0), & \text{if } i \notin \mathcal{E}. \end{cases}$$

We associate a Lagrange multiplier  $\lambda_i$  with equality (14).

By treating the variables  $(\mathbf{l}, \mathbf{u})$  as one block and the variable  $\mathbf{f}$  as the other, we express the updates at the  $(k+1)$ -th iteration below according to the ADMM algorithm.

$$\begin{aligned} (l_i, u_i)^{k+1} &\leftarrow \operatorname{argmin}_{l_i, u_i} \left[ H_i(l_i, u_i) + \frac{\rho}{2} (f_i^k + r_i + l_i - u_i + \frac{\lambda_i^k}{\rho})^2 \right] \\ \mathbf{f}^{k+1} &\leftarrow \operatorname{argmin}_{\mathbf{f} \in \mathcal{F}} \sum_{i=1}^N \left[ F(f_i - \bar{f}) + \frac{\rho}{2} (f_i + r_i + l_i^{k+1} - u_i^{k+1} + \frac{\lambda_i^k}{\rho})^2 \right] \\ \lambda_i^{k+1} &\leftarrow \lambda_i^k + \rho (f_i^{k+1} + r_i + l_i^{k+1} - u_i^{k+1}) \end{aligned}$$

where  $\rho > 0$  is a pre-determined parameter.

To implement the above iteration, each phase updates the controllable power flow  $l_i$ , the net charging and discharging amount  $u_i$ , and the Lagrange multiplier  $\lambda_i$ , while the substation updates the power flow vector  $\mathbf{f}$ . For information exchange, at the  $(k+1)$ -th iteration, the substation sends  $f_i^k$  to each phase, and each phase provides  $m_i^k \triangleq r_i + l_i^{k+1} - u_i^{k+1} + \frac{\lambda_i^k}{\rho}$  to the substation. The schematic representation of the distributed implementation is given in Fig. 2.

**Remark:** Although the communication network structure is the same in both centralized and distributed algorithms (i.e., star topology), with the proposed distributed algorithm, each phase only needs to provide the update of  $m_i^k$  to the substation without revealing the cost functions or other parameters. Therefore, the communication load and the information revealed by each phase are limited.

The convergence behavior of the distributed algorithm is summarized in the following theorem. The proof follows Theorem 2 in [32] and thus is omitted.

*Theorem 2:* Assume that the functions  $D_i(\cdot)$ ,  $C_i(\cdot)$ , and  $F(\cdot)$  are closed, proper, and convex. The sequence  $\{\mathbf{l}^k, \mathbf{u}^k, \mathbf{f}^k, \lambda^k\}$  converges to an optimal primal-dual solution of **P3** with the worst case convergence rate  $O(1/k)$ .

#### IV. EXTENSION TO NON-IDEAL ENERGY STORAGE

In this section, we discuss the algorithm design for non-ideal energy storage with inefficient charging and discharging. This is significant because common storage technologies such as batteries can have round-trip efficiency, i.e.,  $\eta_i^+ \cdot \eta_i^-$ , ranging from 70% to 95% [6].

The mathematical framework of the algorithm design follows that of ideal storage. However, due to imperfect charging

#### Algorithm 2 Centralized algorithm for non-ideal storage.

At time slot  $t$ , the substation executes the following steps sequentially:

- 1: observe the system state  $\mathbf{q}_t$  and the energy state  $s_{i,t}$ ;
- 2: solve **P3'** and obtain an intermediate solution  $\hat{\mathbf{a}}_t \triangleq [\hat{\mathbf{l}}_t, \hat{\mathbf{u}}_t^+, \hat{\mathbf{u}}_t^-, \hat{\mathbf{f}}_t]$ ;
- 3: generate the final solution  $\mathbf{a}_t^*$  where  $u_{i,t}^{+*} = \max\{\hat{u}_{i,t}^+ - \hat{u}_{i,t}^-, 0\}$ ,  $u_{i,t}^{-*} = \max\{\hat{u}_{i,t}^- - \hat{u}_{i,t}^+, 0\}$ ,  $l_{i,t}^* = \hat{l}_{i,t} + \eta_i^- \hat{u}_{i,t}^- - \frac{1}{\eta_i^+} \hat{u}_{i,t}^+ - \eta_i^- u_{i,t}^{-*} + \frac{1}{\eta_i^+} u_{i,t}^{+*}$ , and  $\mathbf{f}_t^* = \hat{\mathbf{f}}_t$ ; and
- 4: update  $s_{i,t}$  by (3) using  $u_{i,t}^{+*}$  and  $u_{i,t}^{-*}$ .

and discharging, the charging and discharging variables  $u_{i,t}^+$  and  $u_{i,t}^-$  cannot be combined into one as we did in Section III, and therefore, the (non-convex) non-simultaneous charging and discharging constraint (2) cannot be eliminated. To overcome this difficulty, we first ignore constraint (2) and then adjust the resultant solution to satisfy the constraint.

Specifically, we first modify the per-slot optimization problem **P3** to the following:

$$\begin{aligned} \mathbf{P3}': \quad &\min_{\mathbf{a}_i} w_t + \sum_{i \in \mathcal{E}} \frac{(s_{i,t} - \beta_i)}{V_i} (u_{i,t}^+ - u_{i,t}^-) \\ &\text{s.t.} \quad (1), (5) - (7) \end{aligned}$$

where we have defined the perturbation parameter

$$\beta_i \triangleq s_{i,\min} + u_{i,\max} + V_i \left( \frac{p_{\max}}{\eta_i^+} + \frac{1}{\eta_i^-} C'_{i,\max} + D'_{i,\max} \right). \quad (15)$$

The parameter  $V_i$  in (15) lies in the interval  $(0, V_{i,\max}]$ , where  $V_{i,\max} \triangleq \frac{s_{i,\max} - s_{i,\min} - 2u_{i,\max}}{\frac{p_{\max}}{\eta_i^+} - p_{\min} \eta_i^- + D'_{i,\max} - D'_{i,\min} + \frac{1}{\eta_i^+} C'_{i,\max} - \eta_i^- C'_{i,\min}}$ .

Note that the definition of  $\beta_i$  in (15) is similar to that in (12) for ideal storage, except the inclusion of the charging and discharging efficiencies. Moreover, if  $\eta_i^+ = \eta_i^- = 1$ , (15) reduces to (12).

The overall centralized algorithm is summarized in Algorithm 2, where we use the superscript notations  $\hat{\cdot}$  and  $\ast$  to indicate the intermediate solution derived from **P3'** and the final solution, respectively. To ensure that the final solution satisfies constraint (2), in Step 3, we adjust the intermediate charging and discharging solutions  $\hat{u}_{i,t}^+$  and  $\hat{u}_{i,t}^-$ , and the controllable power flow  $\hat{l}_{i,t}$ , so that simultaneous charging and discharging cannot happen and the power balance constraint (7) still holds.

**Remarks:** Under some conditions, constraint (2) may automatically hold by solving **P3'**, e.g., when the electricity price  $p_t$  is positive and the cost function of the controllable flow  $C_i(\cdot)$  is increasing. However, if  $p_t$  can be negative or consuming controllable flow costs money, the solution of **P3'** may not meet constraint (2) and thus Step 3 in Algorithm 2 may be necessary. In addition, if simultaneous charging and discharging is allowed in practice, we can simply eliminate Step 3 in Algorithm 2.

The performance of Algorithm 2 is summarized in the following theorem.

*Theorem 3:* Assume that the system state  $\mathbf{q}_t$  is i.i.d. over time and the equipped storage at the phases is not perfectly efficient. Under Algorithm 2 the following statements hold.

- 1)  $\{\mathbf{a}_t^*\}$  is feasible for **P1**.
- 2)  $w^* - w^{\text{opt}} \leq \sum_{i \in \mathcal{E}} \frac{u_{i,\max}^2}{2V_i} + \epsilon$ .
- 3)  $\frac{1}{T} \sum_{t=0}^{T-1} \mathbb{E}[w_t^*] - w^{\text{opt}} \leq \sum_{i \in \mathcal{E}} \left[ \frac{u_{i,\max}^2}{2V_i} + \frac{\mathbb{E}[L(s_i, 0)]}{TV_i} \right] + \epsilon$ ,

where  $\epsilon \triangleq \sum_{i \in \mathcal{E}} p_{\max} u_{i,\max} \left( \frac{1}{\eta_i^+} + \eta_i^- \right) + 2D_{i,\max} + C_{i,\max}$ .

*Proof:* See Appendix F.  $\blacksquare$

The results in Theorem 3 parallel those in Theorem 1 for ideal storage, with an extra gap  $\epsilon$  incurred due to the adjustment of the intermediate solutions. Furthermore, since constraint (2) is ignored in **P3'**, the problem is convex and therefore Algorithm 2 can be implemented distributively using a similar ADMM-based algorithm as that in Section III-B.

## V. NUMERICAL RESULTS

In this section, we numerically evaluate the performance of the proposed algorithm. In each example, all phases are equipped with energy storage. The specific values for the system parameters and functions are shown in Table I. The other default setup is as follows: the system state  $[\mathbf{r}_t, \mathbf{q}_t]$  is i.i.d. over time; at each time slot, the uncontrollable power flows are modeled as independent among phases, and they follow the Gaussian distribution  $\mathcal{N}(0, 4^2)$  truncated within  $[r_{i,\min}, r_{i,\max}]$ ; and the electricity price  $p_t$  is approximated to follow the uniform distribution. For ideal storage, at each time slot, the control action  $\mathbf{a}_t \triangleq [\mathbf{l}_t, \mathbf{u}_t, \mathbf{f}_t]$  is generated by Algorithm 1, and for non-ideal storage,  $\mathbf{a}_t \triangleq [\mathbf{l}_t, \mathbf{u}_t^+, \mathbf{u}_t^-, \mathbf{f}_t]$  is generated by Algorithm 2. Both Algorithms are run for  $T = 500$  time slots. The control parameter  $V_i$  is set to  $V_{i,\max}$ . Note that the only difference between the centralized and the distributed algorithms is whether the per-slot optimization problem in Algorithm 1 (or Algorithm 2) is solved centrally by the substation or in distributed fashion by the substation and all phases. Therefore, both algorithms lead to the same solution to the per-slot optimization problem and thus the same time-averaged system cost.<sup>5</sup>

For comparison, we use a greedy algorithm as the benchmark, which does not account for the future performance. In particular, at each time slot, the greedy algorithm minimizes the current system cost subject to all constraints of **P1**. For ideal storage, the greedy algorithm solves the following optimization problem in each time slot:

$$\begin{aligned} & \min_{\mathbf{l}_t, \mathbf{u}_t, \mathbf{f}_t} w_t \\ & \text{s.t. } (6), (9), (10), \\ & u_{i,t} \geq \max\{-u_{i,\max}, s_{i,\min} - s_{i,t}\} \\ & u_{i,t} \leq \min\{u_{i,\max}, s_{i,\max} - s_{i,t}\}. \end{aligned}$$

For non-ideal storage, at time slot  $t$ , an intermediate solution is first found by solving the optimization problem

$$\min_{\mathbf{l}_t, \mathbf{u}_t^+, \mathbf{u}_t^-, \mathbf{f}_t} w_t \quad \text{s.t. } (1), (3) - (7)$$

without the non-simultaneous charging and discharging constraint (2). Then, the final solution of the greedy algorithm is

<sup>5</sup>Since our focus in this paper is the design of real-time algorithms for storage control, we use a stylized system model. Extending our algorithm to accommodate more details of a power system and implementing the algorithm in a real network using full transient simulation are topics of future work.

TABLE I  
DEFAULT SETUP OF PARAMETERS AND FUNCTIONS

Par.	Setup	Par. (Fun.)	Setup
$[r_{i,\min}, r_{i,\max}]$	$[-8, 8]$ (kW)	$\eta_i^+, \eta_i^-$	1
$[f_{i,\min}, f_{i,\max}]$	$[-5, 5]$ (kW)	$C_i(x)$	$1.5x^2$
$[s_{i,\min}, s_{i,\max}]$	$[2, 10]$ (kWh)	$D_i(x)$	$0.2x^2$
$[p_{\min}, p_{\max}]$	$[7, 12]$ (cents/kWh)	$F(x)$	$10x^2$
$u_{i,\max}$	1 (kW)	N	3

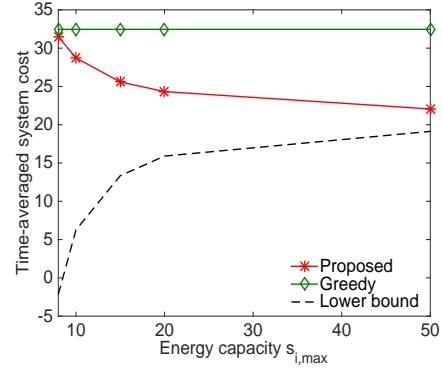


Fig. 3. System cost versus energy capacity of storage ( $s_{1,\max} = s_{2,\max} = s_{3,\max}$ ).

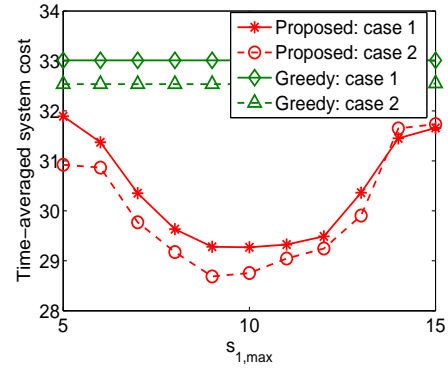


Fig. 4. System cost versus energy capacity of storage at Phase 1 ( $s_{1,\max} + s_{2,\max} + s_{3,\max} = 30$  kWh).

determined by adjusting the intermediate solution using Step 3 in Algorithm 2.

### A. Effect of Energy Capacity of Storage

In this subsection, we consider the effect of energy capacity allocation on the system cost. In Fig. 3, we increase the values of the energy capacity of all storage units from 8 kWh to 50 kWh. Note that for the proposed algorithm the role of  $s_{i,\max}$  is played through the design of the control parameter  $V_{i,\max}$  in (13), and for the greedy algorithm the effect of  $s_{i,\max}$  is reflected through the upper bound of the net charging and discharging variable  $u_{i,t}$  in the optimization problem. We see that, as  $s_{i,\max}$  increases, the system cost of the greedy algorithm does not change, while that of the proposed algorithm drops with a decreasing slope. The former phenomenon could happen when the maximum charging and discharging rate  $u_{i,\max}$  is relatively small and thus  $s_{i,\max}$  has limited effect on  $u_{i,t}$ . The latter observation is consistent with the second remark below Theorem 1 that the proposed

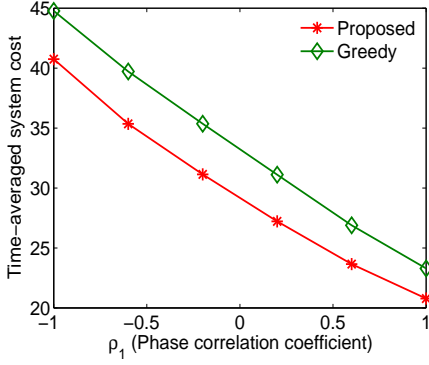


Fig. 5. System cost versus phase correlation coefficient of uncontrollable power flows of Phase 1 and Phase 2.

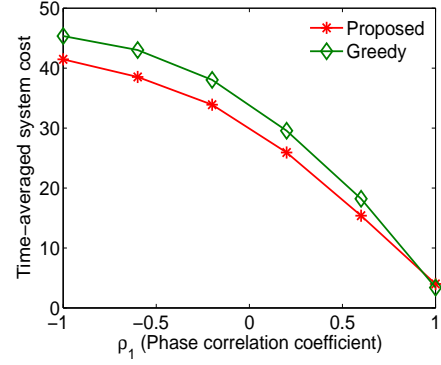


Fig. 6. System cost versus phase correlation coefficient of uncontrollable power flows of Phase 1 and Phases 2, 3.

algorithm is asymptotically optimal when  $s_{i,\max}$  is large. In addition, from Theorem 1.1 we can obtain a lower bound of the minimum system cost as  $w^{\text{opt}} \geq w^* - \sum_{i \in \mathcal{E}} \frac{u_{i,\max}^2}{2V_i}$ . In Fig. 3, we also show the curve of this lower bound. In particular, when the energy capacity is large, this lower bound is tight. However, when the energy capacity is small-to-moderate, this lower bound is loose. For the remaining part of the simulation section, we study the performance of the proposed algorithm when the energy capacity is moderate (e.g.,  $s_{i,\max} = 10$  kWh). Therefore, we have omitted this low bound in the remaining figures. Instead, the benchmark greedy algorithm is more effective in evaluating the numerical performance of the proposed algorithm. Moreover, like the proposed algorithm, the performance of the greedy algorithm serves as an upper bound of the minimum system cost.

In Fig. 4, we fix the total energy capacity of all storage units to 30 kWh (i.e.,  $s_{1,\max} + s_{2,\max} + s_{3,\max} = 30$  kWh) and vary the capacity allocation among phases. In particular, we fix  $s_{2,\max}$  at 10 kWh and change  $s_{1,\max}$  from 5 kWh to 15 kWh. Two cases are considered: Case 1, the standard deviation of the uncontrollable flow of each phase is 4 kW (default setup); Case 2, the standard deviations of the uncontrollable flow of phases 1, 2, and 3 are 3 kW, 4 kW, and 5 kW, respectively. For both algorithms, Case 2 leads to a smaller system cost in general. Moreover, for the greedy algorithm, the system cost barely changes with  $s_{1,\max}$ . In comparison, for the proposed algorithm, the system cost achieves the lowest value when the energy capacity is approximately equally allocated. This observation is consistent with our conclusion in Proposition 2.

### B. Effect of Correlations of Uncontrollable Power Flows

In this subsection, we examine the effect of both the phase and time correlation of the uncontrollable power flows on the system cost. In Fig. 5, we assume that at each time slot, the uncontrollable flows of Phases 1 and 2 are correlated with the phase correlation coefficient, denoted by  $\rho_1$ , while the uncontrollable flow of Phase 3 is independent of those of Phases 1 and 2. We see that, for both algorithms, the system cost decreases with  $\rho_1$ . This is easy to understand, since with a larger  $\rho_1$  the uncontrollable flows of Phases 1 and 2 are more positively related, which makes phase balancing less challenging. In Fig. 6, we additionally assume that the

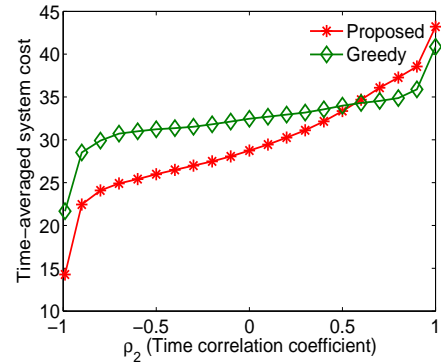


Fig. 7. System cost versus time correlation coefficient of uncontrollable power flow at each phase.

uncontrollable flow of Phase 3 is correlated with that of Phase 1 with the same correlation coefficient  $\rho_1$ . With the additional correlation among phases, the performance gap between the proposed algorithm and the greedy algorithm becomes smaller.

In Fig. 7, we assume that the uncontrollable flows are independent among phases at each time slot, but they are temporally correlated with the time correlation coefficient, denoted by  $\rho_2$ . We observe that, for both algorithms, the system cost increases with  $\rho_2$ . This is because at each phase, when the uncontrollable flow is more positively correlated, the more expensive controllable flow is used for phase balancing since the energy state of the storage is close to its range limit. Consequently, the proposed algorithm achieves a lower system cost when the uncontrollable flow is more negatively correlated.

### C. Effect of Charging and Discharging Circuit Parameters

In Fig. 8, we consider that each phase is equipped with non-ideal energy storage. The charging and discharging efficiencies  $\eta_i^+$  and  $\eta_i^-$  of each storage are assumed to be the same. We see that for both algorithms, the system cost decreases almost linearly with the round-trip efficiency. The decreasing trend is expected since the storage becomes more efficient with a larger value of the round-trip efficiency. In particular, the proposed algorithm leads to a lower system cost when the storage is reasonably efficient. From the figure, this corresponds to the

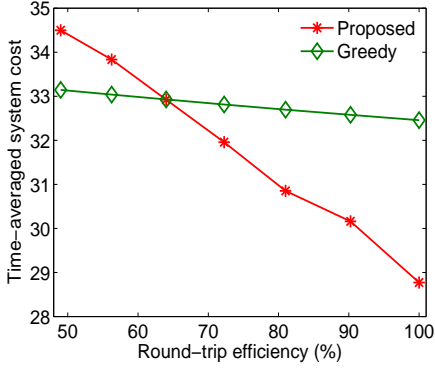


Fig. 8. System cost versus round-trip efficiency of storage at each phase.

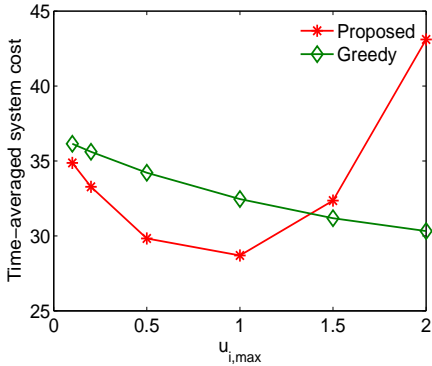


Fig. 9. System cost versus maximum charging/discharging rate of storage at each phase.

case when the round-trip efficiency is greater than 0.65, which includes the range of the round-trip efficiency for most energy storage in practice [6]. On the other hand, when the storage is highly inefficient, the greedy algorithm is shown to produce a better performance.

In Fig. 9, we vary the value of the maximum charging and discharging rate  $u_{i,\max}$  of all storage from 0.1 kW to 3 kW. Note that for the greedy algorithm,  $u_{i,\max}$  only affects the constraints of the net charging and discharging amount, and for the proposed algorithm,  $u_{i,\max}$  additionally affects the design of  $V_{i,\max}$ . We see that, the system cost of the greedy algorithm decreases with  $u_{i,\max}$ , while the system cost of the proposed algorithm first decreases and then increases. For the proposed algorithm, the increasing trend of the system cost could be explained using Theorem 1.1, in which the gap to the optimal objective value increases with  $u_{i,\max}$ . Moreover, from the figure, when  $u_{i,\max}$  is less than 1.5 kW, or, when the charging duration of the storage is larger than 6.6 time units, the proposed algorithm outperforms the greedy one. Since the time scale we consider is seconds to minutes, this is the case for most batteries as the time scale of their charging duration is hours [6]. To improve the algorithm for large  $u_{i,\max}$  is left for the future.

#### D. Effect of Other System Parameters

In Fig. 10, we show the power flow  $f_{i,t}$  between the substation and the  $i$ -th phase as well as their average, for

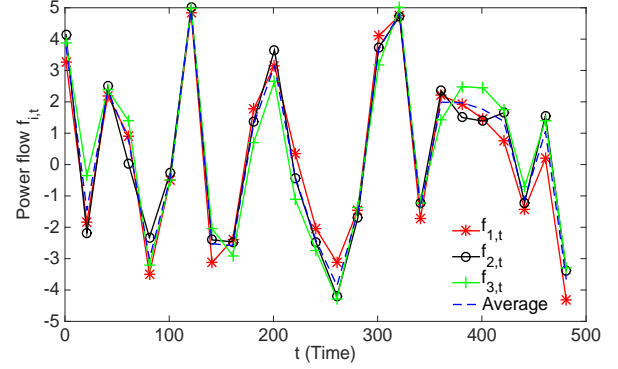


Fig. 10. Time trajectory of power flow  $f_{i,t}$ , for  $i = 1, 2, 3$ .

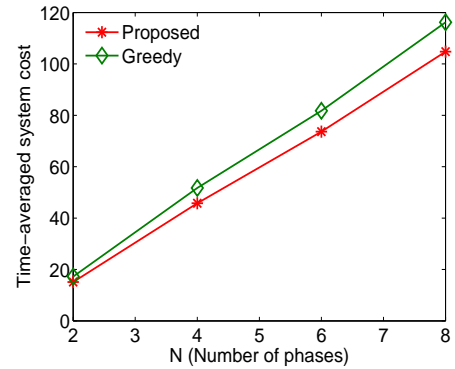


Fig. 11. System cost versus number of total phases.

$i = 1, 2, 3$ . Recall that the purpose of phase balancing is to make  $f_{i,t}$  of all phases as close as possible. The figure shows that the curves of the power flows coincide most of the time. To further narrow the gap of these curves, we can increase the coefficient of the loss function  $F(x)$  so as to impose more penalty for the flow deviation. In return, the system cost would be higher.

Although the three-phase transmission is dominant in practice, we are interested in finding how the number of phases affects the algorithm performance. In Fig. 11, we increase the number of phases  $N$  from 2 to 8. For both algorithms, the system cost grows linearly with  $N$ , which is expected since the system cost sums up the costs of all phases. Moreover, as  $N$  increases, the performance gain of the proposed algorithm over the greedy algorithm increases.

#### E. Convergence of Distributed Implementation

In Fig. 12, we examine the convergence behavior of the distributed algorithm presented in Section III-B for various values of the  $\rho$  parameter. We show the gap between the objective value of a per-slot optimization problem at iteration  $k$  and its minimum objective value over iterations. We see that, for all  $\rho$  values, the gap diminishes at a linear convergence rate. In particular, setting  $\rho = 5$  leads to the best convergence performance. For a moderate accuracy requirement, the iterative procedure can be stopped within 20 iterations. The fast convergence of the proposed algorithm is observed in general

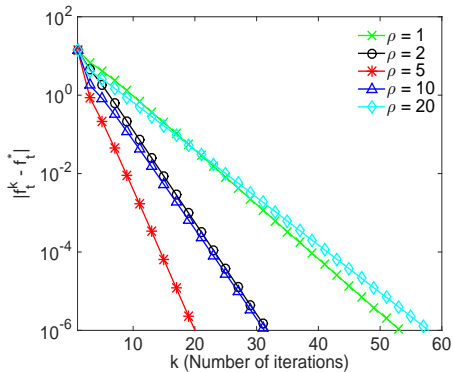


Fig. 12. Performance gap versus number of iterations for distributed algorithm.

with appropriate  $\rho$  values, and we omit the curves of other per-slot optimization problems for brevity.

## VI. CONCLUSION AND FUTURE WORK

We have investigated the problem of phase balancing with energy storage. We have proposed both centralized and distributed real-time algorithms for ideal energy storage and further extended the algorithms to accommodate non-ideal energy storage. Moreover, we have conducted extensive simulation to evaluate the algorithm performance, showing that it can substantially outperform a greedy alternative. Our key conclusions are that positive correlations between the phases make phase balancing easier, and that evenly allocating storage over the phases results in the best performance.

For future work, we are interested in incorporating system statistics into the algorithm design to further improve performance, and also combining energy storage with traditional methods such as feeder reconfiguration for phase balancing.

### APPENDIX A

#### PROOF OF RELAXATION FROM **P1** TO **P2**

Using the energy state update  $s_{i,t+1} = s_{i,t} + u_{i,t}$ , we can derive that the left hand side of constraint (8) equals the following:

$$\lim_{T \rightarrow \infty} \frac{1}{T} \sum_{t=0}^{T-1} \mathbb{E}[u_{i,t}] = \lim_{T \rightarrow \infty} \frac{\mathbb{E}[s_{i,T}]}{T} - \lim_{T \rightarrow \infty} \frac{\mathbb{E}[s_{i,0}]}{T}. \quad (16)$$

In (16), if  $s_{i,t}$  is always bounded, i.e., constraint (4) holds, then the right hand side of (16) equals zero and thus constraint (8) is satisfied. Therefore, **P2** is a relaxed problem of **P1**.

### APPENDIX B

#### AN UPPER BOUND OF THE DRIFT-PLUS-COST FUNCTION

In the following lemma, we show that the drift-plus-cost function is upper bounded.

*Lemma 1:* For all possible decisions and all possible values of  $s_{i,t}$ ,  $i \in \mathcal{E}$ , at each time slot  $t$ , the drift-plus-cost function is upper bounded as follows:

$$\Delta(\mathbf{s}_t) + \mathbb{E}[w_t | \mathbf{s}_t]$$

$$\leq \mathbb{E}[w_t | \mathbf{s}_t] + \sum_{i \in \mathcal{E}} \frac{u_{i,\max}^2}{2V_i} + \frac{s_{i,t} - \beta_i}{V_i} \mathbb{E}[u_{i,t} | \mathbf{s}_t].$$

*Proof:* Based on the definition of  $L(s_{i,t})$  and the update of  $s_{i,t}$ ,

$$\begin{aligned} & L(s_{i,t+1}) - L(s_{i,t}) \\ &= \frac{1}{2} [(s_{i,t+1} - \beta_i)^2 - (s_{i,t} - \beta_i)^2] \\ &\leq (s_{i,t} - \beta_i)u_{i,t} + \frac{1}{2}u_{i,\max}^2. \end{aligned}$$

Using the upper bound above for all phase  $i \in \mathcal{E}$ , taking the conditional expectation, and then adding the term  $\mathbb{E}[w_t | \mathbf{s}_t]$  gives the desired upper bound. ■

### APPENDIX C

#### PROOF OF PROPOSITION 1

Since the per-slot problem **P3** includes all constraints of **P1** except the energy state constraint, the key of the feasibility proof is to show that the energy state  $s_{i,t}$  is bounded within the interval  $[s_{i,\min}, s_{i,\max}]$ . To this end, we first prove the following lemma which gives a sufficient condition for charging or discharging.

*Lemma 2:* Under Algorithm 1, for  $i \in \mathcal{E}$ ,

- 1) if  $s_{i,t} < \beta_i - V_i(p_{\max} + D'_{i,\max} + C'_{i,\max})$ , then  $u_{i,t}^* = u_{i,\max}$ ;
- 2) if  $s_{i,t} > \beta_i - V_i(p_{\min} + D'_{i,\min} + C'_{i,\min})$ , then  $u_{i,t}^* = -u_{i,\max}$ .

*Proof:* For simplicity of notation, we drop the time index  $t$  in **P3**. Using constraint (7) we replace  $l_j$  with  $u_j - f_j - r_j$  in the objective of **P3**. Next we solve **P3** through the partitioning method by first fixing the optimization variables  $\mathbf{f}$  and  $u_j, j \neq i$ , and then minimizing over  $u_i$ . The optimization problem with respect to  $u_i$  is as follows.

$$\min_{u_i} pu_i + D_i(u_i) + C_i(u_i - f_i - r_i) + \frac{(s_i - \beta_i)u_i}{V_i}, \text{ s.t. (11)}$$

The derivative of the objective above with respect to  $u_i$  is  $\frac{\partial(\cdot)}{\partial u_i} = p + D'_i(u_i) + C'_i(u_i - f_i - r_i) + \frac{(s_i - \beta_i)}{V_i}$ . Therefore, if  $s_i$  is upper bounded as shown in Lemma 2.1), we have  $\frac{\partial(\cdot)}{\partial u_i} < 0$  and thus  $u_{i,t}^* = u_{i,\max}$ . Or, if  $s_i$  is lower bounded as shown in Lemma 2.2), we have  $\frac{\partial(\cdot)}{\partial u_i} > 0$  and thus  $u_{i,t}^* = -u_{i,\max}$ . ■

Using Lemma 2 above and the definition of  $\beta_i$ , we can easily show the boundedness of the energy state by mathematical induction, which is omitted here.

### APPENDIX D

#### PROOF OF THEOREM 1

We prove Theorem 1.1 and Theorem 1.2 together. Denote  $\tilde{w}$  as the optimal objective value of **P2**. In the following lemma, we show the existence of a special algorithm for **P2**.

*Lemma 3:* For **P2**, there exists a stationary and randomized solution  $\mathbf{a}_t^s$  that only depends on the system state  $\mathbf{q}_t$ , and at the same time satisfies the following conditions:

$$\mathbb{E}[w_t^s] \leq \tilde{w}, \quad \forall t, \quad \mathbb{E}[u_{i,t}^s] = 0, \quad \forall i \in \mathcal{E}, t,$$

where the expectations are taken over the randomness of the system state and the possible randomness of the actions.

The proof of Lemma 3 follows from Theorem 4.5 in [14] and is omitted for brevity. Using Lemmas 1 and 3, the drift-plus-cost function under Algorithm 1 can be upper bounded as follows:

$$\begin{aligned} & \Delta(\mathbf{s}_t) + \mathbb{E}[w_t^* | \mathbf{s}_t] \\ & \leq \mathbb{E}[w_t^s | \mathbf{s}_t] + \sum_{i \in \mathcal{E}} \left[ \frac{u_{i,\max}^2}{2V_i} + \frac{s_{i,t} - \beta_i}{V_i} \mathbb{E}[u_{i,t}^s | \mathbf{s}_t] \right] \end{aligned} \quad (17)$$

$$\leq \tilde{w} + \sum_{i \in \mathcal{E}} \frac{u_{i,\max}^2}{2V_i} \quad (18)$$

$$\leq w^{\text{opt}} + \sum_{i \in \mathcal{E}} \frac{u_{i,\max}^2}{2V_i} \quad (19)$$

where (17) is derived based on Lemma 1 and the fact that **P3** minimizes the upper bound of the drift-plus-cost function, (18) is derived based on Lemma 3 and the fact that the action  $\mathbf{a}_t^s$  is independent of  $\mathbf{s}_t$ , and the inequality in (19) holds since **P2** is a relaxed problem of **P1**.

Taking expectations over  $\mathbf{s}_t$  on both sides of (19) and summing over  $t \in \{0, \dots, T-1\}$  yields

$$\sum_{i \in \mathcal{E}} \mathbb{E} \left[ \frac{L(s_{i,T}) - L(s_{i,0})}{V_i} \right] + \sum_{t=0}^{T-1} \mathbb{E}[w_t^*] \leq (w^{\text{opt}} + \sum_{i \in \mathcal{E}} \frac{u_{i,\max}^2}{2V_i})T.$$

Note that  $L(s_{i,T})$  is non-negative. Divide both sides of the above inequality by  $T$ . After some arrangement, there is

$$\frac{1}{T} \sum_{t=0}^{T-1} \mathbb{E}[w_t^*] - w^{\text{opt}} \leq \sum_{i \in \mathcal{E}} \left[ \frac{u_{i,\max}^2}{2V_i} + \frac{\mathbb{E}[L(s_{i,0})]}{TV_i} \right], \quad (20)$$

which is the conclusion in Theorem 1.2. Taking lim sup on both sides of (20) gives Theorem 1.1.

## APPENDIX E PROOF OF PROPOSITION 2

Denote  $S$  as the fixed total energy capacity of storage. For simplicity of notation, we drop the index  $i$  when the parameters are the same over all phases or storage units. Given the assumptions in Proposition 2, the optimization problem can be formulated as follows.

$$\begin{aligned} & \min_{s_{i,\max}} \sum_{i \in \mathcal{E}} \frac{u_{\max}^2(p_{\max} - p_{\min} + D'_{\max} - D'_{\min} + C'_{\max} - C'_{\min})}{2(s_{i,\max} - s_{\min} - 2u_{\max})} \\ & \text{s.t.} \quad \sum_{i \in \mathcal{E}} s_{i,\max} = S \end{aligned}$$

where we have replaced  $V_{i,\max}$  with its definition in (13). It can be easily checked that the above problem is a convex optimization problem. Using the Karush-Kuhn-Tucker (KKT) conditions [33], the optimal solutions of  $s_{i,\max}$  must be equal over  $i$ .

## APPENDIX F PROOF OF THEOREM 3

1) To show the feasibility of  $\{\mathbf{a}^*\}$ , it suffices to show that the resultant energy state  $\hat{s}_{i,t}$ ,  $i \in \mathcal{E}$ , is bounded. First we give

sufficient conditions of charging and discharging, which can be shown similarly to Lemma 2.

*Lemma 4:* For  $i \in \mathcal{E}$ ,

- 1) if  $\hat{s}_{i,t} < \beta_i - V_i(\frac{p_{\max}}{\eta_i^+} + D'_{i,\max} + \frac{1}{\eta_i^+} C'_{i,\max})$ , then  $\hat{u}_{i,t}^+ = u_{i,\max}$ ;
- 2) if  $\hat{s}_{i,t} > \beta_i - V_i(p_{\min}\eta_i^- + D'_{i,\min} + \eta_i^- C'_{i,\min})$ , then  $\hat{u}_{i,t}^- = u_{i,\max}$ .

Using Lemma 4 and the mathematical induction arguments, we can show that  $\hat{s}_{i,t} \in [s_{i,\min}, s_{i,\max}]$ ,  $\forall i \in \mathcal{E}$ . Note that the adjustment from  $(\hat{u}_{i,t}^+, \hat{u}_{i,t}^-)$  to  $(\hat{u}_{i,t}^{+*}, \hat{u}_{i,t}^{-*})$  does not change the difference  $\hat{u}_{i,t}^+ - \hat{u}_{i,t}^-$ . Therefore, the resultant energy state  $s_{i,t}^*$  equals  $\hat{s}_{i,t}$  and thus is bounded within  $[s_{i,\min}, s_{i,\max}]$ .

2) We prove Theorem 3.2 and Theorem 3.3 together. Similar to the ideal case, the relaxed problem of **P1** can be formed as follows.

$$\begin{aligned} \mathbf{P2}': \quad & \min_{\{\mathbf{a}_t\}} \limsup_{T \rightarrow \infty} \frac{1}{T} \sum_{t=0}^{T-1} \mathbb{E}[w_t] \\ & \text{s.t.} \quad (1), (5), (6), (7), \\ & \quad \quad \quad \lim_{T \rightarrow \infty} \frac{1}{T} \sum_{t=0}^{T-1} \mathbb{E}[u_{i,t}^+ - u_{i,t}^-] = 0, \forall i \in \mathcal{E}. \end{aligned}$$

Denote the optimal value of **P2'** by  $\tilde{w}'$ . We first give the following two lemmas, which can be shown similarly to Lemmas 1 and 3.

*Lemma 5:* For all possible decisions and all possible values of  $s_{i,t}$ ,  $i \in \mathcal{E}$ , in each time slot  $t$ , the drift-plus-cost function is upper bounded as follows

$$\begin{aligned} \Delta(\mathbf{s}_t) + \mathbb{E}[w_t | \mathbf{s}_t] & \leq \sum_{i \in \mathcal{E}} \frac{u_{i,\max}^2}{2V_i} + \mathbb{E}[w_t | \mathbf{s}_t] \\ & \quad + \sum_{i \in \mathcal{E}} \frac{s_{i,t} - \beta_i}{V_i} \mathbb{E}[u_{i,t}^+ - u_{i,t}^- | \mathbf{s}_t]. \end{aligned} \quad (21)$$

*Lemma 6:* For **P2'**, there exists a stationary and randomized solution  $\mathbf{a}_t^s$  that only depends on the system state  $\mathbf{q}_t$ , and at the same time satisfies the following conditions:

$$\mathbb{E}[w_t^s] \leq \tilde{w}', \quad \forall t, \quad (22)$$

$$\mathbb{E}[u_{i,t}^{+s} - u_{i,t}^{-s}] = 0, \quad \forall i \in \mathcal{E}, t. \quad (23)$$

Denote the optimal values of **P3'** under  $\hat{\mathbf{a}}_t$  and the adjusted solution  $\mathbf{a}_t^*$  by  $\hat{g}_t$  and  $g_t^*$ , respectively. In the following lemma, we characterize the gap between  $\hat{g}_t$  and  $g_t^*$ .

*Lemma 7:* Under the proposed algorithm, at each time  $t$  we have  $g_t^* - \hat{g}_t \leq \epsilon$ , where  $\epsilon \triangleq \sum_{i \in \mathcal{E}} p_{\max} u_{i,\max} (\frac{1}{\eta_i^+} + \eta_i^-) + 2D_{i,\max} + C_{i,\max}$ .

*Proof:* Using the objective of **P3'**, we have

$$\begin{aligned} & g_t^* - \hat{g}_t \\ & \leq \sum_{i \in \mathcal{E}} p_t \left( \frac{1}{\eta_i^+} u_{i,t}^{+*} - \eta_i^- u_{i,t}^{-*} \right) + D_i(u_{i,t}^{+*}) + D_i(-u_{i,t}^{-*}) + C_i(l_{i,t}^*) \\ & \quad - p_t \left( \frac{1}{\eta_i^+} \hat{u}_{i,t}^+ - \eta_i^- \hat{u}_{i,t}^- \right) - D_i(\hat{u}_{i,t}^+) - D_i(-\hat{u}_{i,t}^-) - C_i(\hat{l}_{i,t}) \\ & \leq \sum_{i \in \mathcal{E}} p_t \frac{1}{\eta_i^+} u_{i,t}^{+*} + p_t \eta_i^- \hat{u}_{i,t}^- + D_i(u_{i,t}^{+*}) + D_i(-u_{i,t}^{-*}) + C_i(l_{i,t}^*) \\ & \leq \epsilon. \end{aligned}$$

Using Lemmas 5, 6, and 7, the drift-plus-penalty function can be further upper bounded as follows.

$$\begin{aligned}
& \Delta(\mathbf{s}_t^*) + \mathbb{E}[w_t^* | \mathbf{s}_t^*] \\
& \leq \mathbb{E}[\hat{w}_t | \mathbf{s}_t^*] + \sum_{i \in \mathcal{E}} \left[ \frac{u_{i,\max}^2}{2V_i} + \frac{s_{i,t}^* - \beta_i}{V_i} \mathbb{E}[\hat{u}_{i,t}^+ - \hat{u}_{i,t}^- | \mathbf{s}_t^*] \right] + \epsilon \\
& \leq \mathbb{E}[w_t^s | \mathbf{s}_t^*] + \sum_{i \in \mathcal{E}} \left[ \frac{u_{i,\max}^2}{2V_i} + \frac{s_{i,t}^* - \beta_i}{V_i} \mathbb{E}[\hat{u}_{i,t}^{+s} - \hat{u}_{i,t}^{-s} | \mathbf{s}_t^*] \right] + \epsilon \\
& \leq \epsilon + \sum_{i \in \mathcal{E}} \frac{u_{i,\max}^2}{2V_i} + \tilde{w}' \\
& \leq \epsilon + \sum_{i \in \mathcal{E}} \frac{u_{i,\max}^2}{2V_i} + w^{\text{opt}}.
\end{aligned}$$

The remaining proof is similar to that for Theorem 1 and is omitted for brevity.

## REFERENCES

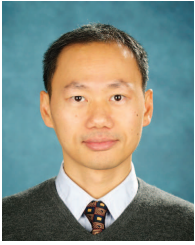
- [1] A. Meier, *Electric Power Systems: A Conceptual Introduction*. Wiley-IEEE Press, 2006.
- [2] G. Putrus, P. Suwanapongkarl, D. Johnston, E. Bentley, and M. Narayana, "Impact of electric vehicles on power distribution networks," in *Proc. IEEE VPPC*, Sep. 2009.
- [3] J. Zhu, M. Chow, and F. Zhang, "Phase balancing using mixed-integer programming," *IEEE Trans. Power Syst.*, vol. 13, no. 4, pp. 1487–1492, Nov 1998.
- [4] Y. Hsu, Y. Hwu, S. Liu, Y. Chen, H. Feng, and Y. Lee, "Transformer and feeder load balancing using a heuristic search approach," *IEEE Trans. Power Syst.*, vol. 8, no. 1, pp. 184–190, Feb. 1993.
- [5] P. Denholm, E. Ela, B. Kirby, and M. Milligan, "The role of energy storage with renewable electricity generation," National Renewable Energy Laboratory, Tech. Rep., Jan. 2010.
- [6] A. Castillo and D. Gayme, "Grid-scale energy storage applications in renewable energy integration: A survey," *Energy Convers. Manage.*, vol. 87, pp. 885–894, Aug. 2014.
- [7] R. Green II, L. Wang, and M. Alam, "The impact of plug-in hybrid electric vehicles on distribution networks: A review and outlook," *RENEW SUST ENERG REV*, vol. 15, no. 1, p. 544553, Jan. 2011.
- [8] H. Hao, B. Sanandaji, K. Poolla, and T. Vincent, "A generalized battery model of a collection of thermostatically controlled loads for providing ancillary service," in *Communication, Control, and Computing (Allerton), Annual Allerton Conference on*, Oct. 2013.
- [9] —, "Aggregate flexibility of thermostatically controlled loads," *IEEE Trans. Power Syst.*, 2014.
- [10] A. Nayyar, J. A. Taylor, A. Subramanian, D. S. Callaway, and K. Poolla, "Aggregate flexibility of collections of loads," in *Proc. IEEE CDC*, Dec. 2013.
- [11] H. Su and A. Gamal, "Modeling and analysis of the role of energy storage for renewable integration: Power balancing," *IEEE Trans. Power Syst.*, vol. 28, no. 4, pp. 4109–4117, Nov. 2013.
- [12] J. Taylor, D. Callaway, and K. Poolla, "Competitive energy storage in the presence of renewables," *IEEE Trans. Power Syst.*, vol. 28, no. 2, pp. 985–996, May 2013.
- [13] D. Zhu and G. Hug, "Decomposed stochastic model predictive control for optimal dispatch of storage and generation," *IEEE Trans. Smart Grid*, vol. 5, no. 4, pp. 2044–2053, Jul. 2014.
- [14] M. Neely, *Stochastic Network Optimization with Application to Communication and Queueing Systems*. Morgan & Claypool, 2010.
- [15] R. Uргаonkar, B. Uргаonkar, M. Neely, and A. Sivasubramaniam, "Optimal power cost management using stored energy in data centers," in *Proc. ACM SIGMETRICS*, 2011.
- [16] S. Sun, M. Dong, and B. Liang, "Real-time power balancing in electric grids with distributed storage," *IEEE J. Sel. Topics Signal Process.*, vol. 8, no. 6, pp. 1167–1181, Dec. 2014.
- [17] —, "Real-time welfare-maximizing regulation allocation in dynamic aggregator-EVs system," *IEEE Trans. Smart Grid*, vol. 5, no. 3, pp. 1397–1409, May 2014.

- [18] L. Huang, J. Walrand, and K. Ramchandran, "Optimal demand response with energy storage management," in *Proc. IEEE SmartGridComm*, Nov. 2012.
- [19] Y. Guo, M. Pan, Y. Fang, and P. Khargonekar, "Decentralized coordination of energy utilization for residential households in the smart grid," *IEEE Trans. Smart Grid*, vol. 4, no. 3, pp. 1341–1350, Sep. 2013.
- [20] Q. Li, T. Cui, R. Negi, F. Franchetti, and M. Ilić, "On-line decentralized charging of plug-in electric vehicles in power systems." [Online]. Available: <http://arxiv.org/abs/1106.5063>
- [21] S. Lakshminarayana, T. Quek, and H. Poor, "Cooperation and storage tradeoffs in power-grids with renewable energy resources," *IEEE J. Sel. Areas Commun.*, 2014.
- [22] J. Qin, Y. Chow, J. Yang, and R. Rajagopal, "Online modified greedy algorithm for storage control under uncertainty," Jun. 2014. [Online]. Available: <http://arxiv.org/abs/1405.7789>
- [23] —, "Distributed online modified greedy algorithm for networked storage operation under uncertainty," Jun. 2014. [Online]. Available: <http://arxiv.org/pdf/1406.4615v2.pdf>
- [24] M. Alam, K. Muttaqi, and D. Sutanto, "Community energy storage for neutral voltage rise mitigation in four-wire multigrounded LV feeders with unbalanced solar PV allocation," to appear in *IEEE Trans. Smart Grid*.
- [25] C. Bennett, R. Stewart, and J. Lu, "Development of a three-phase battery energy storage scheduling and operation system for low voltage distribution networks," *Appl. Energy*, vol. 146, pp. 122–134, May 2015.
- [26] S. Sun, J. Taylor, M. Dong, and B. Liang, "Distributed real-time phase balancing for power grids with energy storage," in *Proc. ACC*, Jul. 2015.
- [27] W. Kersting, *Distribution System Modeling and Analysis*, 3rd ed. CRC Press LLC, 2012.
- [28] P. Ramadass, B. Haran, R. White, and B. Popov, "Performance study of commercial LiCoO2 and spinel-based Li-ion cells," *J. Power Sources*, vol. 111, no. 2, pp. 210–220, Apr. 2002.
- [29] A. Wood, B. Wollenberg, and G. Sheblé, *Power Generation, Operation, and Control*, 3rd ed. Wiley-Interscience, 2013.
- [30] C. Thraupoulidis, S. Bose, and B. Hassibi, "Optimal placement of distributed energy storage in power networks," to appear in *IEEE Trans. Autom. Control*.
- [31] S. Boyd, N. Parikh, E. Chu, B. Peleato, and J. Eckstein, *Distributed Optimization and Statistical Learning via the Alternating Direction Method of Multipliers*. Found. Trends Mach. Learning, 2011.
- [32] H. Wang and A. Banerjee, "Online alternating direction method." [Online]. Available: <http://arxiv.org/abs/1306.3721>
- [33] S. Boyd and L. Vandenberghe, *Convex Optimization*. Cambridge University Press, 2004.



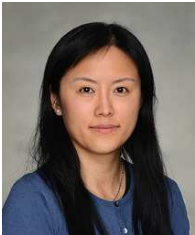
**Sun Sun** (S'11) received the B.S. degree in Electrical Engineering and Automation from Tongji University, Shanghai, China, in 2005. From 2006 to 2008, she was a software engineer in the Department of GSM Base Transceiver Station of Huawei Technologies Co. Ltd.. She received the M.Sc. degree in Electrical and Computer Engineering from University of Alberta, Edmonton, Canada, in 2011. Now, she is pursuing her Ph.D. degree in the Department of Electrical and Computer Engineering of University of Toronto, Toronto, Canada. Her current

research interest lies in the areas of stochastic optimization, distributed control, learning, and economics, with the application of renewable generation, energy storage, demand response, and power system operations.



**Ben Liang** (S'94-M'01-SM'06) received honors-simultaneous B.Sc. (valedictorian) and M.Sc. degrees in Electrical Engineering from Polytechnic University in Brooklyn, New York, in 1997 and the Ph.D. degree in Electrical Engineering with a minor in Computer Science from Cornell University in Ithaca, New York, in 2001. In the 2001-2002 academic year, he was a visiting lecturer and post-doctoral research associate with Cornell University. He joined the Department of Electrical and Computer Engineering at the University of Toronto in

2002, where he is now a Professor. His current research interests are in mobile communications and networked systems. He has served as an editor for the IEEE Transactions on Communications, an editor for the IEEE Transactions on Wireless Communications, and an associate editor for the Wiley Security and Communication Networks journal, in addition to regularly serving on the organizational and technical committees of a number of conferences. He is a senior member of IEEE and a member of ACM and Tau Beta Pi.



**Min Dong** (S'00-M'05-SM'09) received the B.Eng. degree from Tsinghua University, Beijing, China, in 1998, and the Ph.D. degree in electrical and computer engineering with minor in applied mathematics from Cornell University, Ithaca, NY, in 2004. From 2004 to 2008, she was with Corporate Research and Development, Qualcomm Inc., San Diego, CA. In 2008, she joined the Department of Electrical, Computer and Software Engineering at University of Ontario Institute of Technology, Ontario, Canada, where she is currently an Associate Professor. She

also holds a status-only Associate Professor appointment with the Department of Electrical and Computer Engineering, University of Toronto since 2009. Her research interests are in the areas of statistical signal processing for communication networks, cooperative communications and networking techniques, and stochastic network optimization in dynamic networks and systems.

Dr. Dong received the Early Researcher Award from Ontario Ministry of Research and Innovation in 2012, the Best Paper Award at IEEE ICC in 2012, and the 2004 IEEE Signal Processing Society Best Paper Award. She was an Associate Editor for the IEEE SIGNAL PROCESSING LETTERS during 2009-2013, and currently serves as an Associate Editor for the IEEE TRANSACTIONS ON SIGNAL PROCESSING. She has been an elected member of IEEE Signal Processing Society Signal Processing for Communications and Networking (SP-COM) Technical Committee since 2013.



**Joshua A. Taylor** (M'11) received the B.S. degree from Carnegie Mellon University in 2006, and the S.M. and Ph.D. degrees from the Massachusetts Institute of Technology in 2008 and 2011, all in Mechanical Engineering. From 2011 to 2012, he was a postdoctoral researcher in Electrical Engineering and Computer Sciences at the University of California, Berkeley. He is currently an assistant professor in the Department of Electrical and Computer Engineering and the associate director of the Institute for Sustainable Energy at the University of Toronto. His current

research interests include renewable energy and demand response, machine learning, and infrastructural couplings.